Engineering a humanized animal model of polycythemia vera with minimal *JAK2*V617F mutant allelic burden

Polycythemia vera (PV) is a chronic myeloproliferative neoplasm (MPN) characterized by the overproduction of red blood cells. Over 95% of PV patients' disease is driven by the *JAK2*V617F mutation. While *JAK2*V617F mutant mouse models have provided mechanistic insights into PV biology, most of these models present a mutant cell burden much higher than the variant allele frequency (VAF) of *JAK2*V617F found in PV patients. Thus, current PV mouse models result in a limited understanding of the earliest stages of PV development including what is the minimal mutant cell burden required for disease manifestation. In order to circumvent these limitations, we developed an engineered model of PV utilizing CRISPR/Cas9 homology-directed repair (HDR) to introduce a *JAK2*V6717F mutation into the endogenous locus of human CD34$^+$ cells. Xenografting targeted cells into NSGS mice recapitulated human PV pathologies *in vivo*. We used this tool to address two questions: (i) what is the minimum mutant VAF needed to generate PV pathologies, and (ii) does the developmental context of the cell of origin influence disease trajectory of MPN. This model provides a valuable preclinical tool to test new PV therapies *in vivo* and an alternative model to study the development and progression of PV when primary patient samples are limited or unavailable.

Myeloproliferative neoplasms (MPN) are driven by somatic mutations acquired in hematopoietic stem and progenitor cells (HSPC), characterized by the deviant proliferation of one or more myeloid lineages.[1,2] MPN can present as polycythemia vera (PV; excess erythrocytes), essential thrombocythemia (ET; excess platelets), or myelofibrosis (MF; bone marrow fibrosis). The *JAK2*V617F mutation is a recurrent driver of MPN.[3-5] However, the burden of *JAK2*V617F mutant cells varies widely in patients and can induce clinical phenotypes with very low VAF.[6,7] In PV, over 95% of patients have *JAK2*V617F as the driving pathogenic mutation, but the mutation burden can be below 3% VAF in some patients.[8] It is not clear how such a low mutant cell burden can generate MPN pathologies. Current *JAK2*V617F mouse modeling strategies utilize retroviral transduction,[9,10] transgenic alleles,[11] or genetic knock-in (KI) models.[12,13] However, most of these models yield high *JAK2*V617F mutational frequencies that do not accurately reflect the clonal trajectory of PV patients. In order to overcome the limitations of mouse models, we recently developed methods to transplant CD34$^+$ cells from MPN patients to generate patient-derived xenografts (PDX). In the case of MF, xenografting patient-derived CD34$^+$ cells is able to propagate the genotypes, phenotypes and key patient pathologies such as reticulin fibrosis in PDX.[14] However, attempts to generate PDX from PV patients has been less successful, with poor engraftment and limited numbers of CD34$^+$ cells obtainable from the blood of these patients. In order to circumvent these issues, here we describe a novel model to study development of human PV employing CRISPR/Cas9 methodology to introduce the *JAK2*V6717F mutation into the endogenous locus of HSPC obtained from human cord blood (CB) or healthy bone marrow (BM; *Online Supplementary Figure S1A*).

For a pilot feasibility study, CB-derived CD34$^+$ cells were nucleofected with CRISPR/Cas9 reagents to introduce the *JAK2*V617F (="VF") mutation into the endogenous locus. For a negative control, a single-stranded oligo donor nucleotide (ssODN) was designed to introduce a silent mutation at the same amino acid, such that there is no resulting protein change (*JAK2*V617V ="VV") but a single base genetic variant that serves as a trackable barcode. This engineered system was tested by xenografting a high input of 80,000 nucleofected CD34$^+$ CB cells. KI efficiency was 13-14% for both VF and VV variants (*Online Supplementary Figure S1B*). There was high human engraftment in both VF and VV groups in peripheral blood (PB; *Online Supplementary Figure S1C*) and BM (*Online Supplementary Figure S1D*). *JAK2*V617F cells exhibited increased engraftment in the spleen (*Online Supplementary Figure S1E*), splenomegaly (*Online Supplementary Figure S1F*) and propagation of the mutation in the BM (*Online Supplementary Figure S1G*).

In order to model PV driven by low *JAK2*V617F mutant allele burden, we utilized the KI strategy but with a significantly lower cell input. We also sought to examine how the *JAK2*V617F mutation can lead to distinct MPN pathologies by testing the hypothesis that developmental context of the cell of origin influences the disease trajectory. CD34$^+$ cells from CB and adult BM (donor ages =32, 39 years) were nucleofected as above (Figure 1A) and 20,000 nucleofected cells were transplanted intra-tibially into sub-lethally irradiated (2.5 Gy) NSGS mice. *JAK2*V617F and *JAK2*V617V donor cells were present at low frequencies in the PB of both recipient groups (Figure 1B, C). The myeloid lineage compartment was increased in hCD45$^+$ PB cells in mice that received the *JAK2*V617F mutant HSPC derived from either BM or CB compared to *JAK2*V617V controls (Figure 1D). Mice transplanted with *JAK2*V617F mutant HSPC from both CB and BM donors displayed increased hematocrit, hemoglobin, and platelet counts, suggestive of a PV-like phenotype (Figure 1E). WBC counts were not significantly different (Figure 1E). Flow cytometric discrimination between human- and mouse-derived erythrocytes showed mice receiving VF cells exhibited a higher percentage of human red blood cells (*Online Supplementary Figure S2A*). Interestingly, between weeks 16 and 24 post-transplant, certain recipients of BM-derived *JAK2*V617F cells displayed a marked decrease in hematocrit, hemoglobin, and platelet counts (Figure 1E),

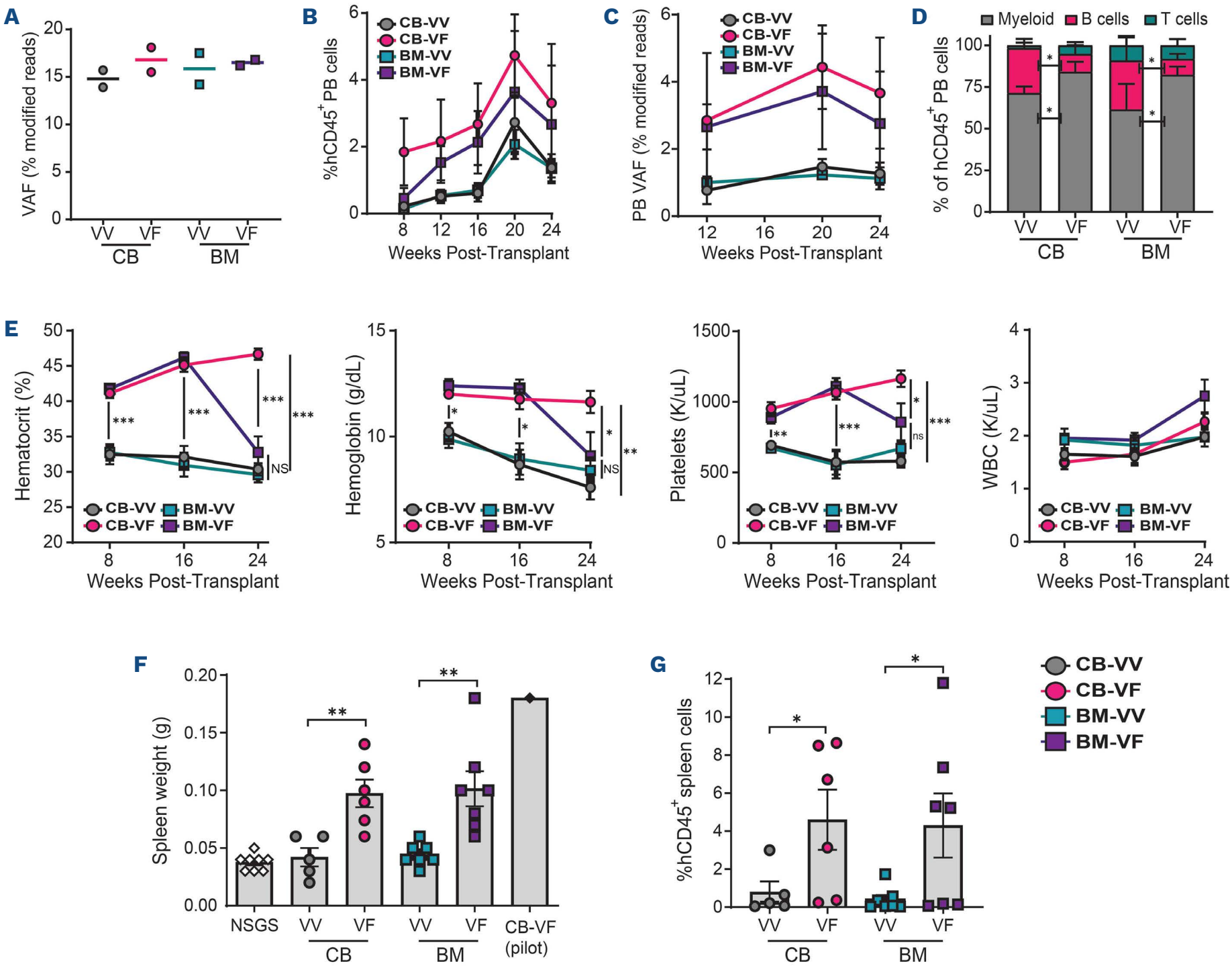

Figure 1. Engineering a humanized model of polycythemia vera. (A) Knock-in efficiency of VF and VV mutations in CD34⁺ cells of indicated source determined by next-generation sequencing. (B) Engraftment of human cells in the peripheral blood of NSGS mice determined by flow cytometry. (C) Variant allele frequency (VAF) of engineered mutations in the peripheral blood (PB) of NSGS mice determined by digital droplet plolymerase chain reaction. (D) Lineage distribution of engrafted human CD45⁺ cells in the PB of NSGS mice. (E) Blood counts of indicated recipient groups across the experimental time course. (F) Spleen weights of mice receiving indicated human cells. (G) Engraftment of human cells in the spleens of NSGS mice. N=5-7 mice per group, data are compiled from 2 independent experiments. *P<0.05, **P<0.01, ***P<0.001. Mean ± standard error of the mean values are shown. NSGS: age-matched irradiated non-transplanted mice; WBC: white blood cells; BM: bone marrow; CB: cord blood; VF: *JAK2*V617F; VV: *JAK2*V617V.

potentially suggestive of disease progression from PV to MF. Spleen weights and human cell engraftment in the spleen were increased in both *JAK2*V617F cohorts (Figure 1F, G), representative of the splenomegaly often present in MPN patients.

Human cell engraftment in the BM mirrored that of the PB (Figure 2A), although overall cellularity was increased in CB-derived *JAK2*V617F recipients (*Online Supplementary Figure S2B*). Again, the myeloid lineage in the BM was increased in the groups which received *JAK2*V617F-derived cells (Figure 2B). Parallel flow cytometric analysis on mouse (m)CD45⁺ BM cells from the same mice showed there were no changes in mouse blood cell lineages between any cohort, suggesting that any observed effect was driven by transplanted human-derived cells (*Online Supplementary Figure S2C*). Human HSC (hCD45⁺, mCD45⁻, Lineage⁻ [CD3/14/16/19/20/56], CD34⁺, CD38⁻, CD45RA⁻, CD90⁺; *Online Supplementary Figure S2D*) were detected in both CB- and BM-derived *JAK2*V617F cohorts, but not *JAK2*V617V recipients (Figure 2C), consistent with our prior studies showing that normal human HSC do not self-renew in the inflammatory environment of NSGS BM.[14] *JAK2*V617F-mutant BM cells showed increased phosphorylation of STAT3 and STAT5, a canonical feature of MPN patients (Figure 2D). Thus, in addition to reproducibly

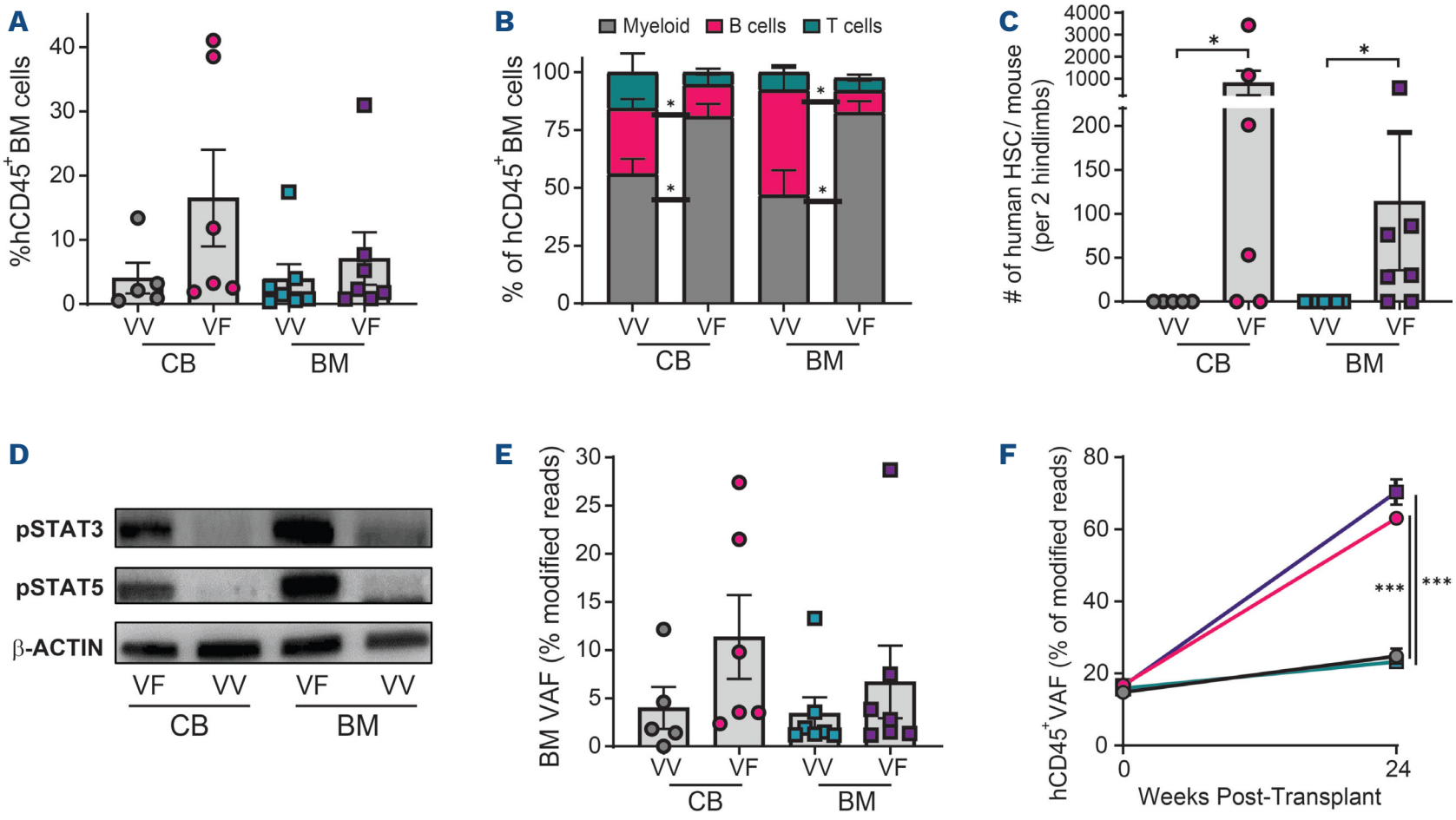

Figure 2. Manifestation of polycythemia vera pathologies from a minimal *JAK2*V617F mutant allele burden. (A) Engraftment of human cells in the bone marrow (BM) of NSGS mice. (B) Lineage distribution of engrafted human CD45+ cells in the BM of NSGS mice. (C) Absolute number of human hematopoietic stem cells (HSC) in BM of NSGS recipient mice for each donor group. (D) Western blot analysis showing activation of the JAK/STAT pathway in VF targeted cells. (E) Variant allele frequency (VAF) of engineered mutations in BM of NSGS mice determined by digital droplet polymerase chain reaction. (F) VAF of engineered mutations specifically within human cell fractions. N=5-7 mice per group, data are compiled from 2 independent experiments. *P<0.05, ***P<0.001. Mean ± standard error of the mean values are shown. NSGS: age-matched irradiated non-transplanted mice; CB: cord blood; VF: *JAK2*V617F; VV: *JAK2*V617V.

generating hallmark MPN pathologies (*Online Supplementary Figure S3*), this system also produces characteristic molecular features of *JAK2*V617F-mutant MPN.

Six months post-transplant, VAF was determined by droplet digital polymerase chain reaction (ddPCR) in whole BM and purified hCD45+ cells from the BM of xenografted mice as previously described.[15] The VAF of *JAK2*V617F in whole BM essentially mirrored overall engraftment (Figure 2E). Within the hCD45+ BM cells, the VAF of VV-targeted cells remained relatively consistent over the transplant period. In contrast, there was a significant increase in the VAF of VF-targeted cells (Figure 2F), demonstrating a competitive advantage for *JAK2*V617F-mutant clones.

Reticulin staining of the BM revealed fibrosis in the majority of recipients of BM-derived VF-edited cells (5/7), which was not observed in recipients of CB-derived cells edited with the *JAK2*V617F mutation (Figure 3A). No reticulin fibrosis was detected in any recipients of *JAK2*V617V control cells (Figure 3B). Histopathology showed the BM from VF-targeted recipients displayed increased megakaryocytes (Figure 3C). Several BM-derived *JAK2*V617F recipients had distinctive histopathology, presenting dysmorphic (hyper-lobated, staghorn, and/or cloud-like nuclei) and/or multinucleated (distinct, multinucleated nuclei amidst increased cytoplasm) megakaryocytes (Figure 3D). Dysmorphic megakaryocytes were significantly increased in recipients transplanted with *JAK2*V617F-edited cells from either CB or BM, whereas multinucleated megakaryocytes were almost exclusively associated with BM-derived *JAK2*V617F cells (Figure 3E). The frequency of multinucleated megakaryocytes strongly correlated with the degree of reticulin fibrosis in the BM (Figure 3F). Moreover, in BM-derived VF recipients, fibrosis grade correlated with decreasing hematocrit and increased spleen weight (Figure 3F). These pathologies are suggestive of disease progression from PV to MF. This engineered system presents a unique opportunity to study the molecular mechanisms that promote MPN that may lead to these distinct disease trajectories.

In conclusion, we present an engineered humanized *JAK2*V617F KI system wherein a minority of mutant HSPC initiate MPN in the background of normal hematopoiesis. A burden of mutant cells at low VAF (<5%) was able to induce classical MPN pathologies in NSGS mice, mimicking early-stage human PV. However, it should be noted that due to differences in the biology of NSGS mice, the MPN pathologies are not precise recapitulations of human patients or some genetic mouse models of MPN derived in C57Bl/6 backgrounds. While hematocrit was elevated in NSGS recipients of VF-edited cells, it was markedly lower than that observed in PV patients.

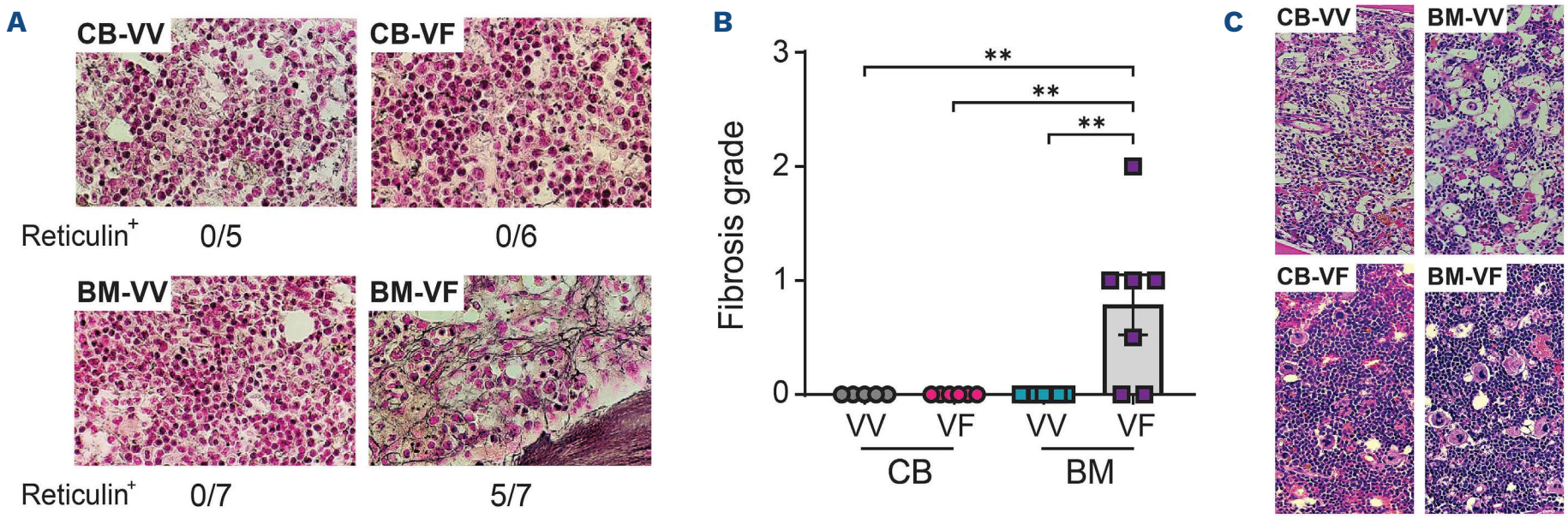

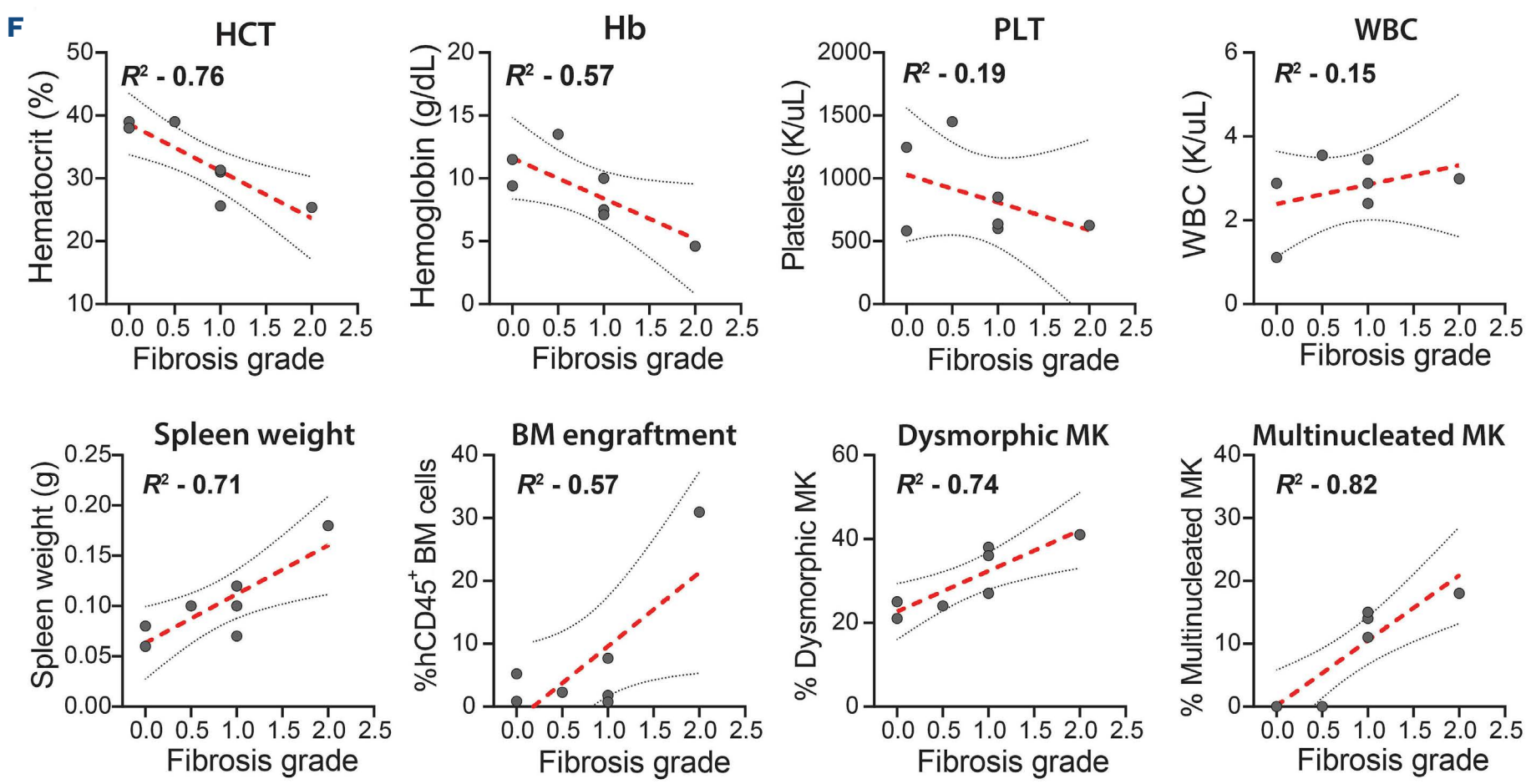

Continued on following page.

Figure 3. Histopathology of xenografted mice. (A) Representative bone marrow (BM) sections of NSGS mice from indicated groups showing reticulin staining. (B) Quantification of the degree of reticulin fibrosis in BM of recipient mice from indicated groups. (C) Representative histological images of BM sections of NSGS mice from indicated recipient groups. (D) Histopathology showing multinucleated megakaryocytes (MK) in BM of a mouse receiving BM-derived *JAK2V617F* targeted cells. (E) Quantification of the percentage of dysmorphic and multinucleated MK in the BM of recipient mice from indicated groups. (F) Correlations of BM reticulin fibrosis grade with pathological parameters (non-linear regression) for recipients transplanted with BM-derived *JAK2*V617F-targeted cells. Line of best fit (red) and 95% confidence intervals are shown. N=5-7 mice per group, data are compiled from 2 independent experiments. **P*<0.05, ****P*<0.001. Mean ± standard error of the mean values are shown. NSGS: age-matched irradiated non-transplanted mice; CB: cord blood; HCT: hematocrit; WBC: white blood cells; Hb: hemoglobin; Plt: platelets; MK: megakaryocytes; VF: *JAK2*V617F; VV: *JAK2*V617V.

Similarly, while splenomegaly was observed, it was not to the same relative degree that can occur in MPN patients. Despite these limitations, this model represents a robust and reproducible tool for the investigation of *JAK2*V617F mutant clone fitness and provides a platform for preclinical testing of novel PV interventions. Moreover, the majority of the cohort receiving BM-derived VF-mutated CD34$^+$ cells developed reticulin fibrosis at 6 months. At present, there is no mouse model that reliably models the transformation of PV to MF that we present here in a humanized system.

Authors

Tyler M. Parsons, Aishwarya Krishnan, Wangisa M.B. Dunuwille, Andrew L. Young, Jason Arand, Wentao Han and Grant A. Challen

Division of Oncology, Department of Medicine, Washington University School of Medicine, St. Louis, MO, USA

Correspondence:
G.A. CHALLEN - grantchallen@wustl.edu

https://doi.org/10.3324/haematol.2023.283858

Received: June 30, 2023.
Accepted: September 15, 2023.
Early view: September 28, 2023.

Disclosures

GAC acts as a consultant and received research funding from Incyte, Ajax Therapeutics and ReNAgade Therapeutics Management not relevant to this work. ALY acts as a consultant for BioGenerator not relevant to this work. TMP acts as a consultant for Pillar Patient Advocates and the MPN Research Foundation not relevant to this work. The remaining authors have no conflicts of interest to disclose.

Contributions

GAC, TMP and ALY developed the concept and designed the study. TMP, AK, WMBD, WH and JA performed experiments and acquired data. TMP and GAC analyzed data. GAC acquired funding. TMP and GAC carried out project administration and supervised the project.

Acknowledgments

We thank Dr. Marianna Ruzinova (Washington University School of Medicine) for pathological scoring of reticulin fibrosis and all members of the Challen Laboratory for ongoing contributions and critical discussion. We thank the Washington University Musculoskeletal Histology and Morphometry Core for histology, and the Siteman Cancer Center Flow Cytometry core for cell sorting and analysis.

Funding

The Siteman Cancer Center Flow Cytometry core is supported by NIH Cancer Center Support Grant P30CA091842. This work was supported by the National Institutes of Health (HL147978, CA236819 and DK124883) and Research Scholar Grant CSCC-RSG-23-991417-01-CSCC from the American Cancer Society and the Lisa Dean Moseley Foundation (to GAC). TMP is a fellow of the Leukemia and Lymphoma Society. ALY was supported by NIH T32HL007088. GAC is a scholar of the Leukemia and Lymphoma Society.

Data-sharing statement

Data and protocols are available upon request to the corresponding author.

References

1. Grabek J, Straube J, Bywater M, Lane SW. MPN: the molecular drivers of disease initiation, progression and transformation and their effect on treatment. Cells. 2020;9(8):1901.
2. Kleppe M, Levine RL. New pieces of a puzzle: the current biological picture of MPN. Biochim Biophys Acta. 2012;1826(2):415-422.
3. Levine RL, Wadleigh M, Cools J, et al. Activating mutation in the tyrosine kinase JAK2 in polycythemia vera, essential thrombocythemia, and myeloid metaplasia with myelofibrosis. Cancer Cell. 2005;7(4):387-397.
4. Baxter EJ, Scott LM, Campbell PJ, et al. Acquired mutation of the tyrosine kinase JAK2 in human myeloproliferative disorders. Lancet. 2005;365(9464):1054-1061.
5. Kralovics R, Passamonti F, Buser AS, et al. A gain-of-function mutation of JAK2 in myeloproliferative disorders. N Engl J Med. 2005;352(17):1779-1790.

6. Limvorapitak W, Parker J, Hughesman C, McNeil K, Foltz L, Karsan A. No differences in outcomes between JAK2 V617F–positive patients with variant allele fraction < 2% versus 2-10%: a 6-year province-wide retrospective analysis. Clin Lymphoma Myeloma Leuk. 2020;20(9):e569-e578.
7. Moliterno AR, Kaizer H, Reeves BN. JAK2V617F allele burden in polycythemia vera: burden of proof. Blood. 2023;141(16):1934-1942.
8. Perricone M, Polverelli N, Martinelli G, et al. The relevance of a low JAK2 V617F allele burden in clinical practice: a monocentric study. Oncotarget. 2017;8(23):37239-37249.
9. Lacout C, Pisani DF, Tulliez M, Gachelin FM, Vainchenker W, Villeval JL. JAK2V617F expression in murine hematopoietic cells leads to MPD mimicking human PV with secondary myelofibrosis. Blood. 2006;108(5):1652-1660.
10. Wernig G, Mercher T, Okabe R, Levine RL, Lee BH, Gilliland DG. Expression of Jak2V617F causes a polycythemia vera-like disease with associated myelofibrosis in a murine bone marrow transplant model. Blood. 2006;107(11):4274-4281.
11. Xing S, Wanting TH, Zhao W, et al. Transgenic expression of JAK2V617F causes myeloproliferative disorders in mice. Blood. 2008;111(10):5109-5117.
12. Marty C, Lacout C, Martin A, et al. Myeloproliferative neoplasm induced by constitutive expression of JAK2V617F in knock-in mice. Blood. 2010;116(5):783-787.
13. Mullally A, Lane SW, Ball B, et al. Physiological Jak2V617F expression causes a lethal myeloproliferative neoplasm with differential effects on hematopoietic stem and progenitor cells. Cancer Cell. 2010;17(6):584-596.
14. Celik H, Krug E, Zhang CR, et al. A humanized animal model predicts clonal evolution and therapeutic vulnerabilities in myeloproliferative neoplasms. Cancer Discov. 2021;11(12):3126-3141.
15. Wiley B, Parsons TM, Burkart S, et al. Effect of clonal hematopoiesis on cardiovascular disease in people living with HIV. Exp Hematol. 2022;114:18-21.